Computational light scattering (PAP315)

Lecture 2

Karri Muinonen[1,2]

Professor of Astronomy

[1]Department of Physics, University of Helsinki, Finland

[2]Finnish Geospatial Research Institute (FGI), Masala, Finland

Contents

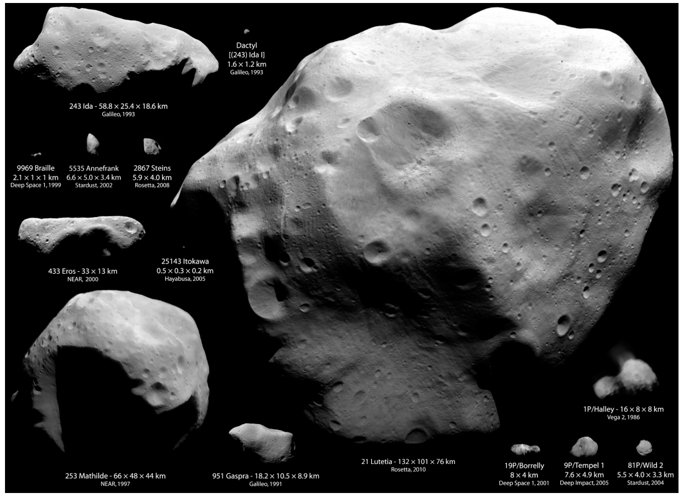

- Introduction
- Multiple scattering
  - Numerical methods
  - Radiative transfer and coherent backscattering (RT-CB)
  - Radiative transfer with reciprocal transactions (R^2T^2)
- Validation of numerical methods
  - Discrete media of spherical particles
  - Discrete media of nonspherical particles
- Astrophysical Scattering Laboratory
  - Scatterometer
  - Spectropolarimetric goniometer
  - Integrating-sphere spectrometer
- Application to asteroids and comets
- Conclusions

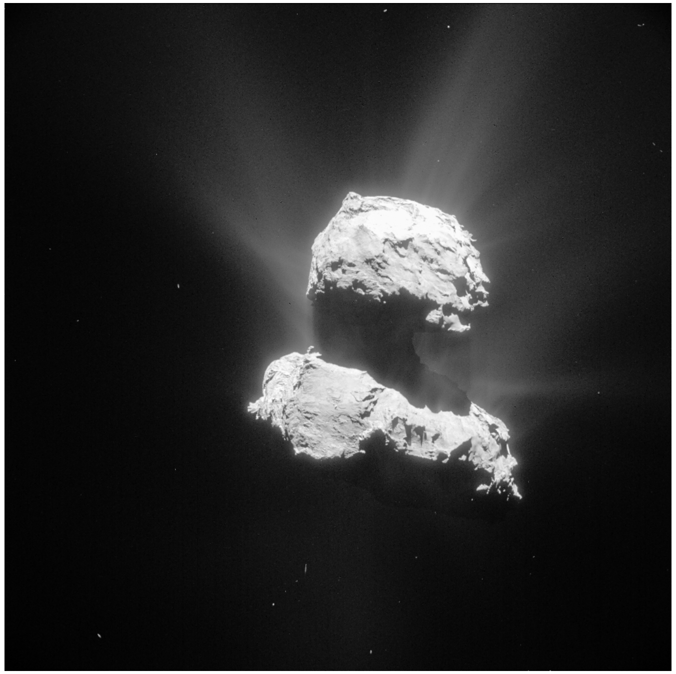

Introduction

- Physical characterization of the surfaces of airless planetary objects
- Direct problem of light scattering by discrete random media of particles with varying particle size, shape, refractive index, and volume density
- Inverse problem based on astronomical observations and/or experimental measurements
- Plane of scattering, scattering angle, solar phase angle, degree of linear polarization

Polarimetric & photometric observations

Moon

Photometry

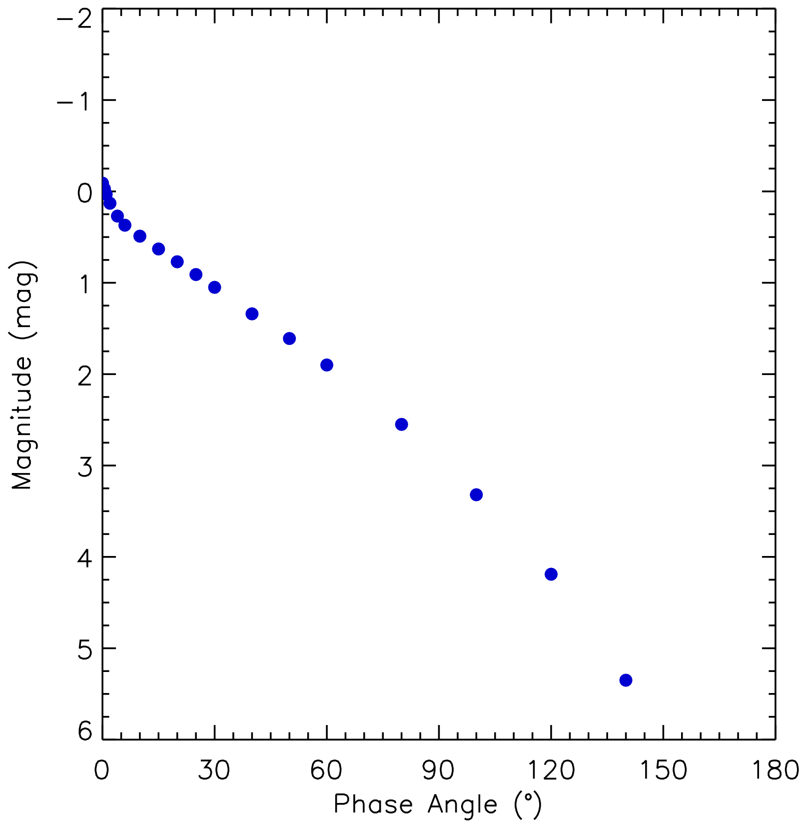

Polarimetry

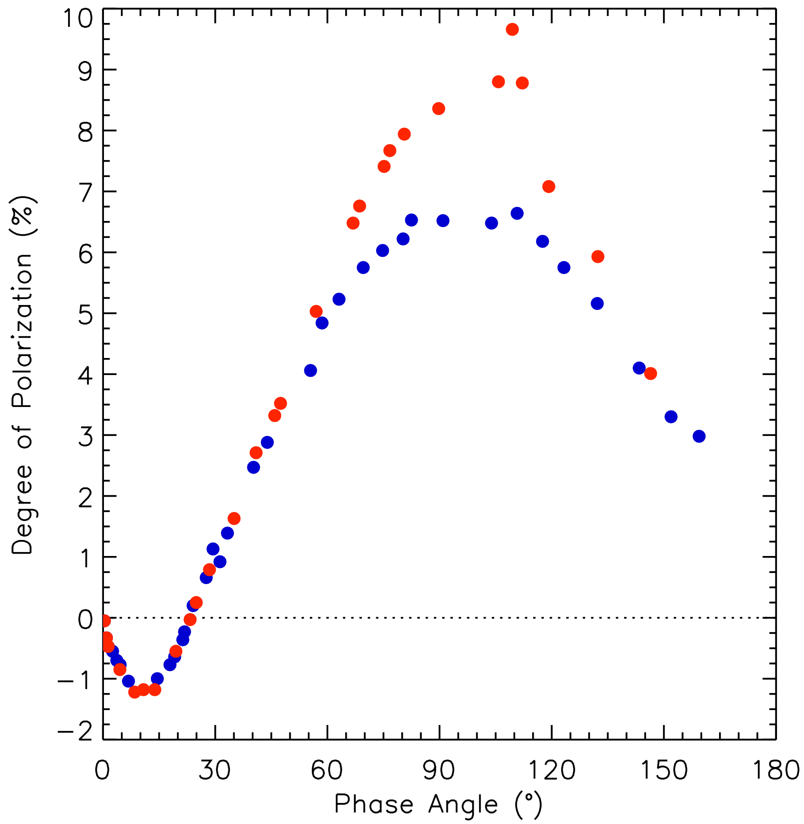

Rougier (1933), Lyot (1929)

Asteroids

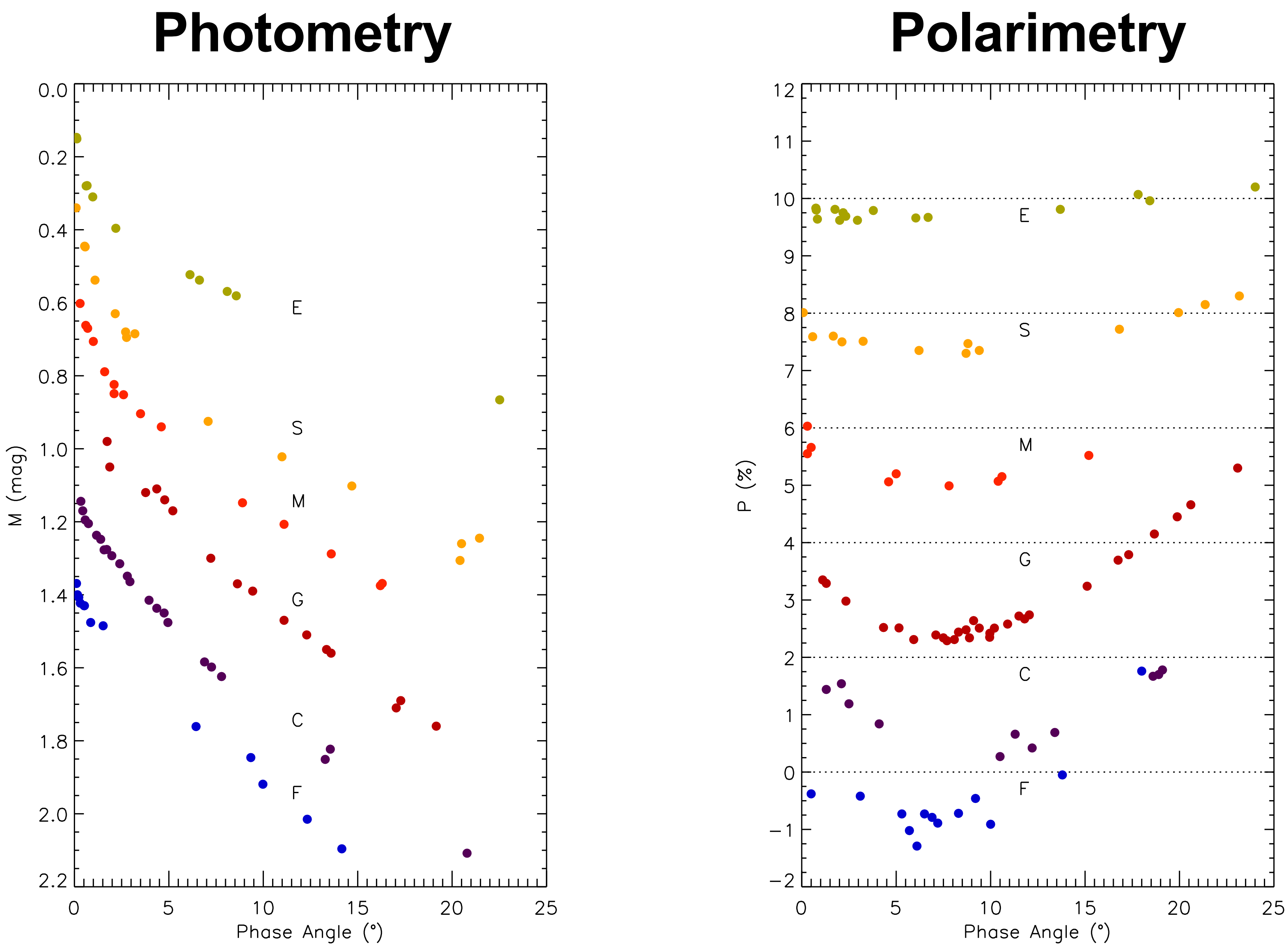

Muinonen et al., in Polarimetry of Stars and Planetary Systems, 2016 (obs. ref. therein)

Asteroid spectropolarimetry

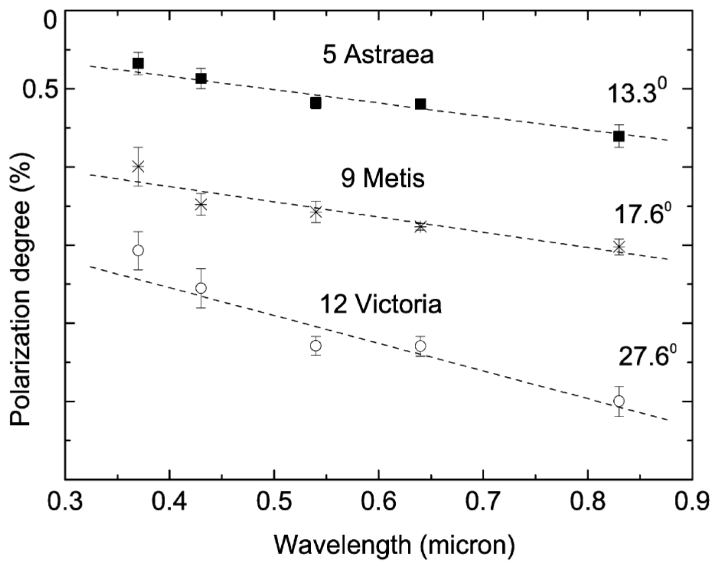

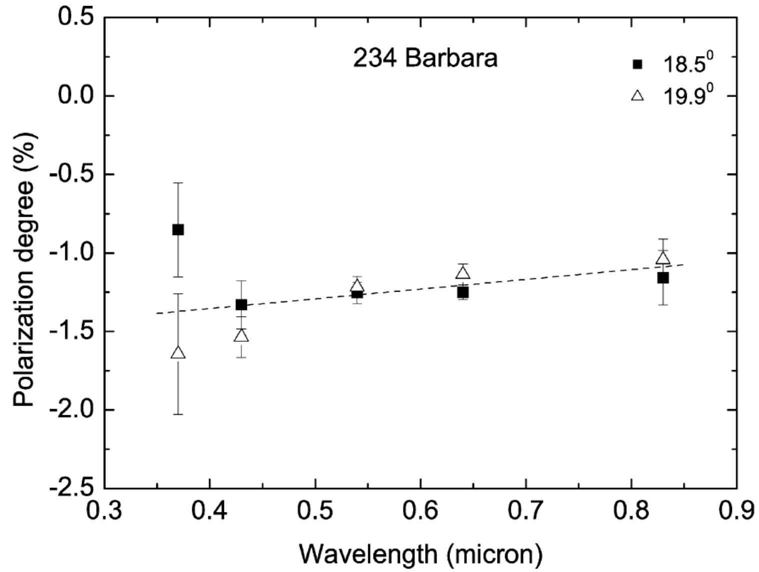

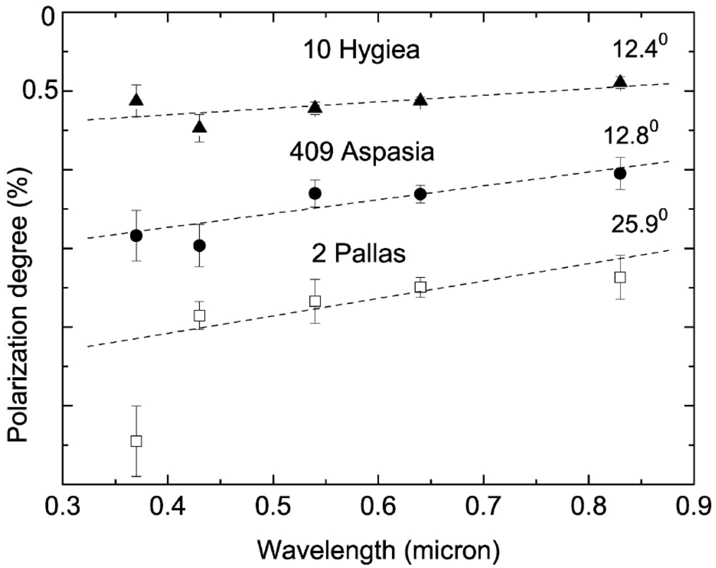

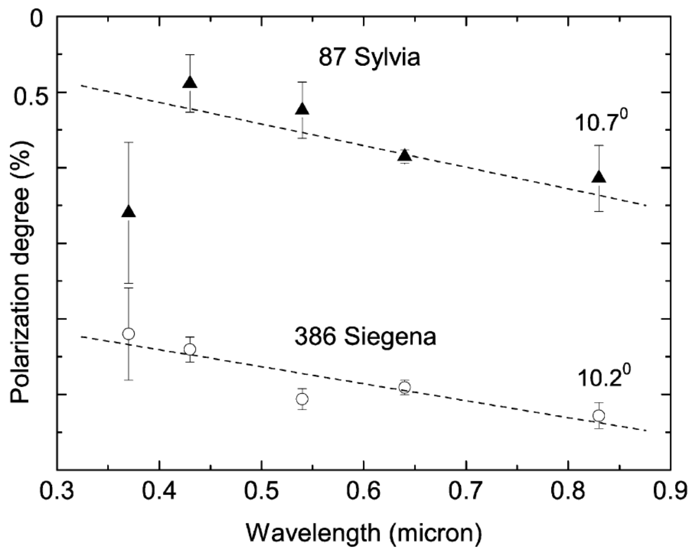

Belskaya et al. 2009

Asteroid spectropolarimetry

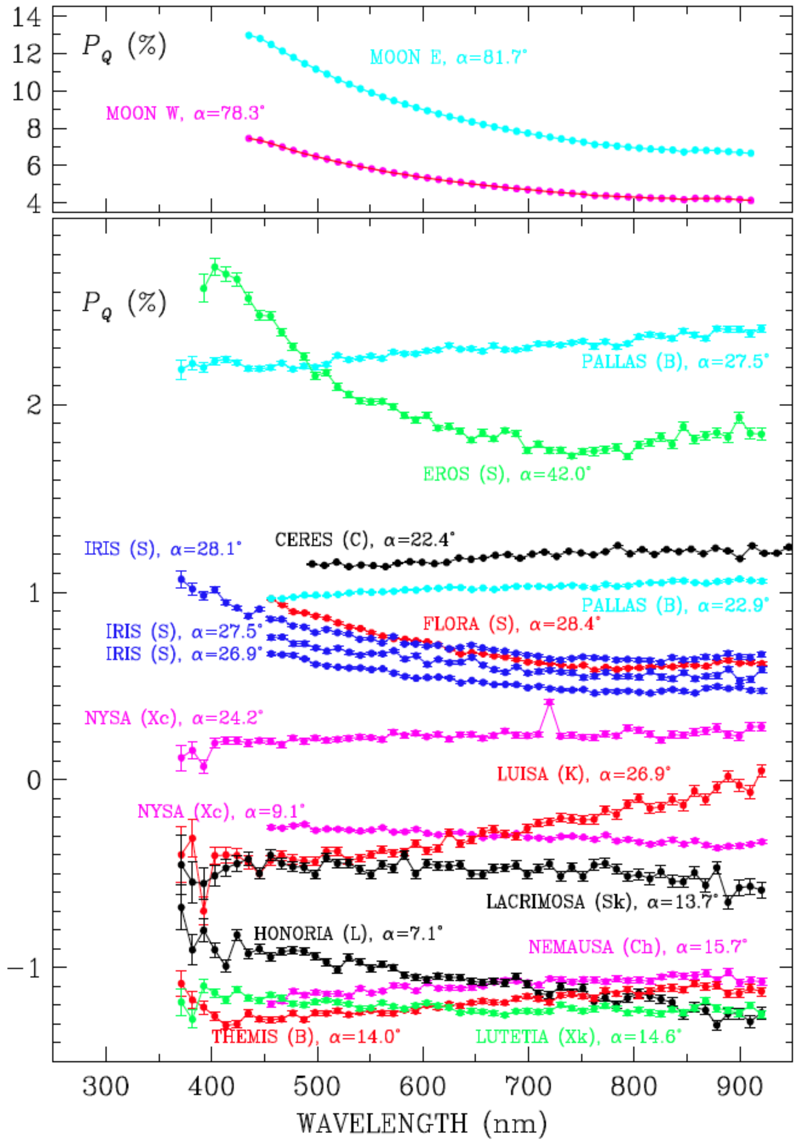

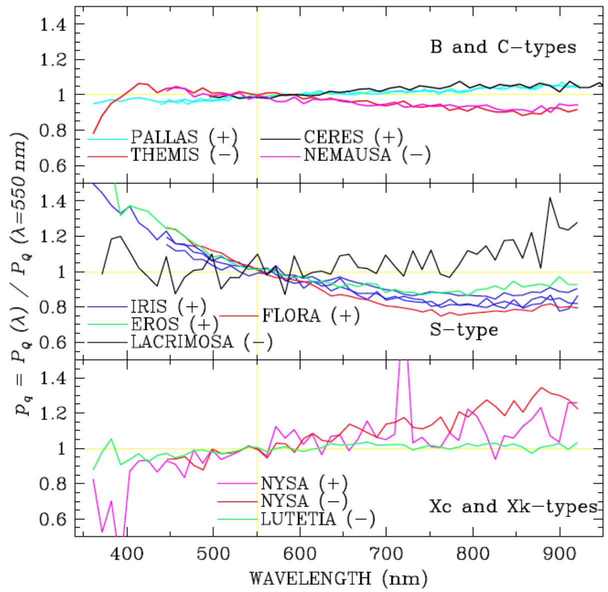

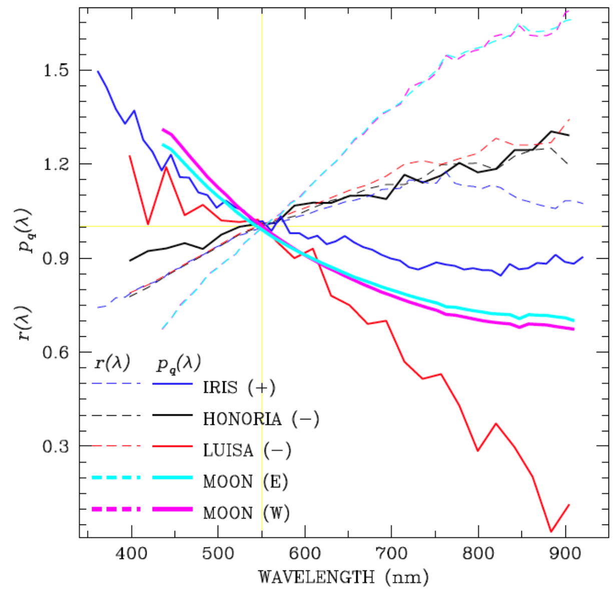

Bagnulo et al. 2015

Saturn's Rings

Photometry

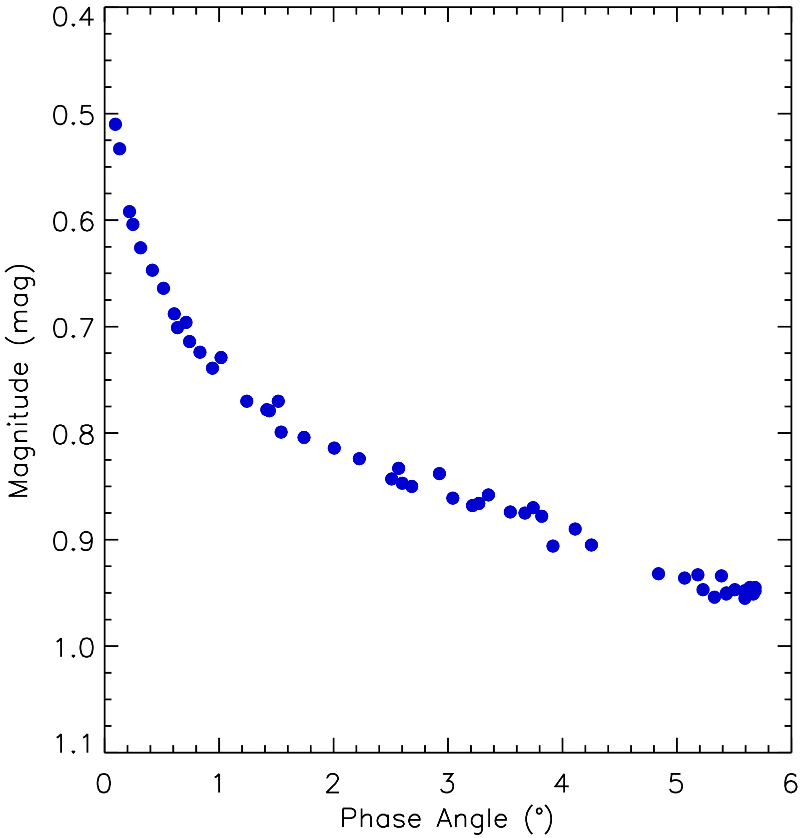

Polarimetry

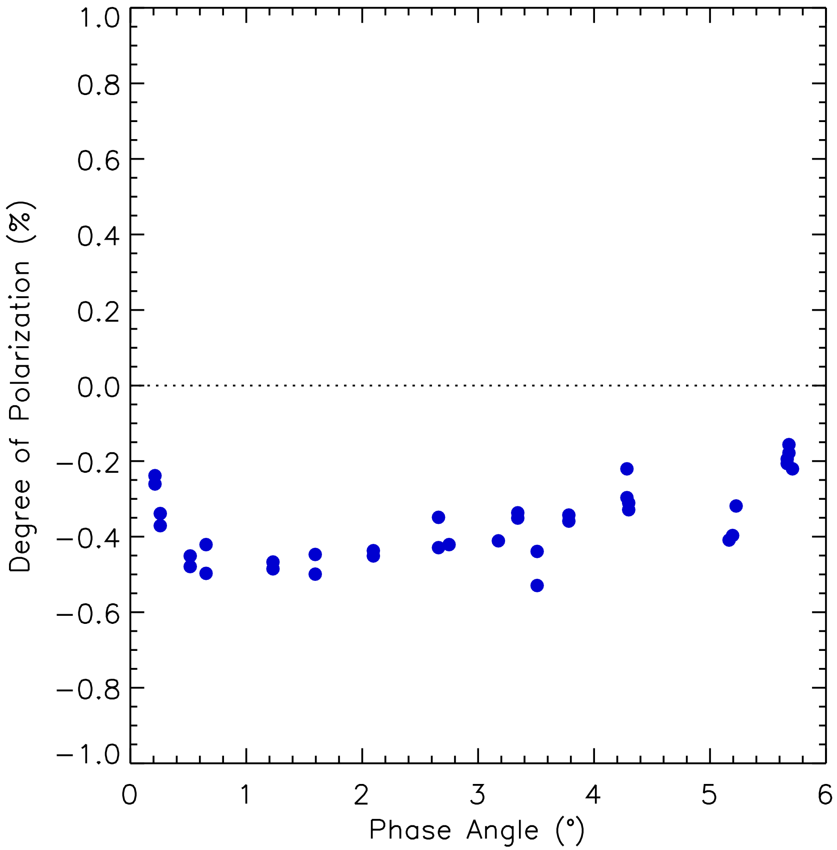

Transneptunian objects (TNOs)

Polarimetry for large TNOs

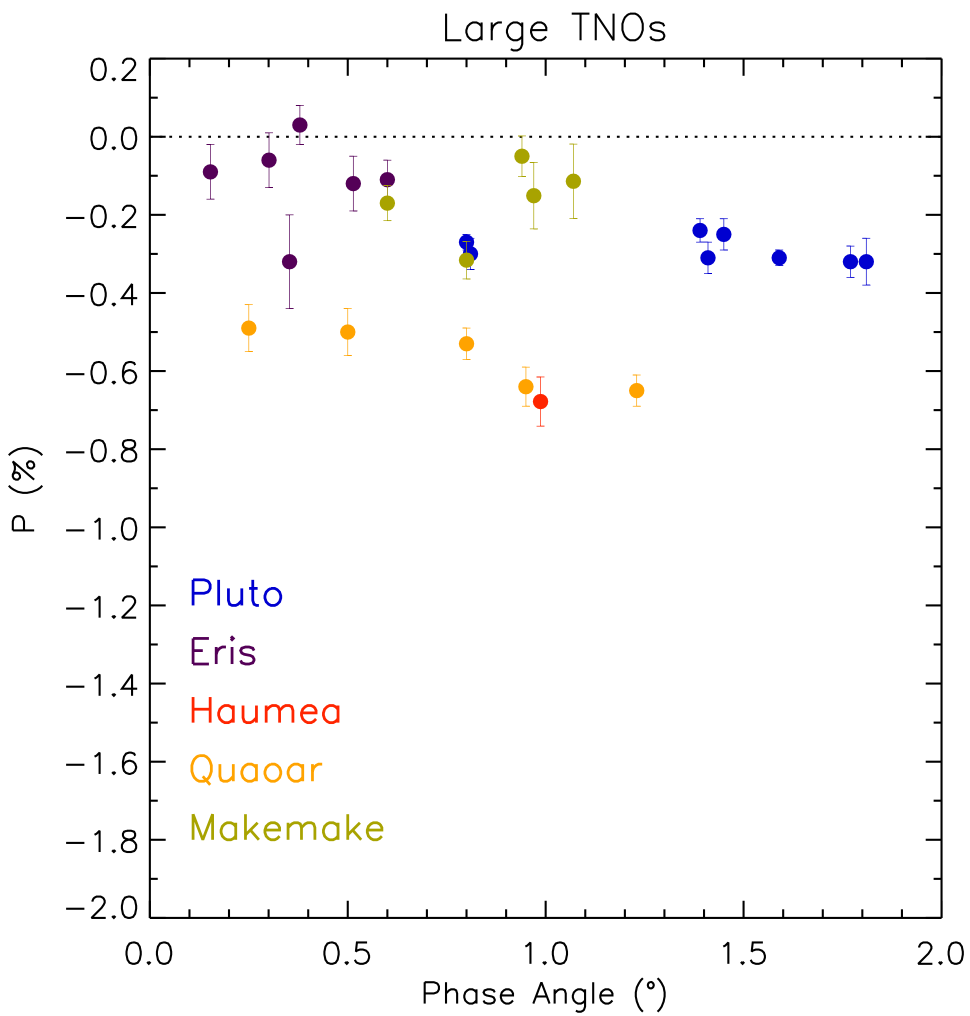

Polarimetry for small TNOs

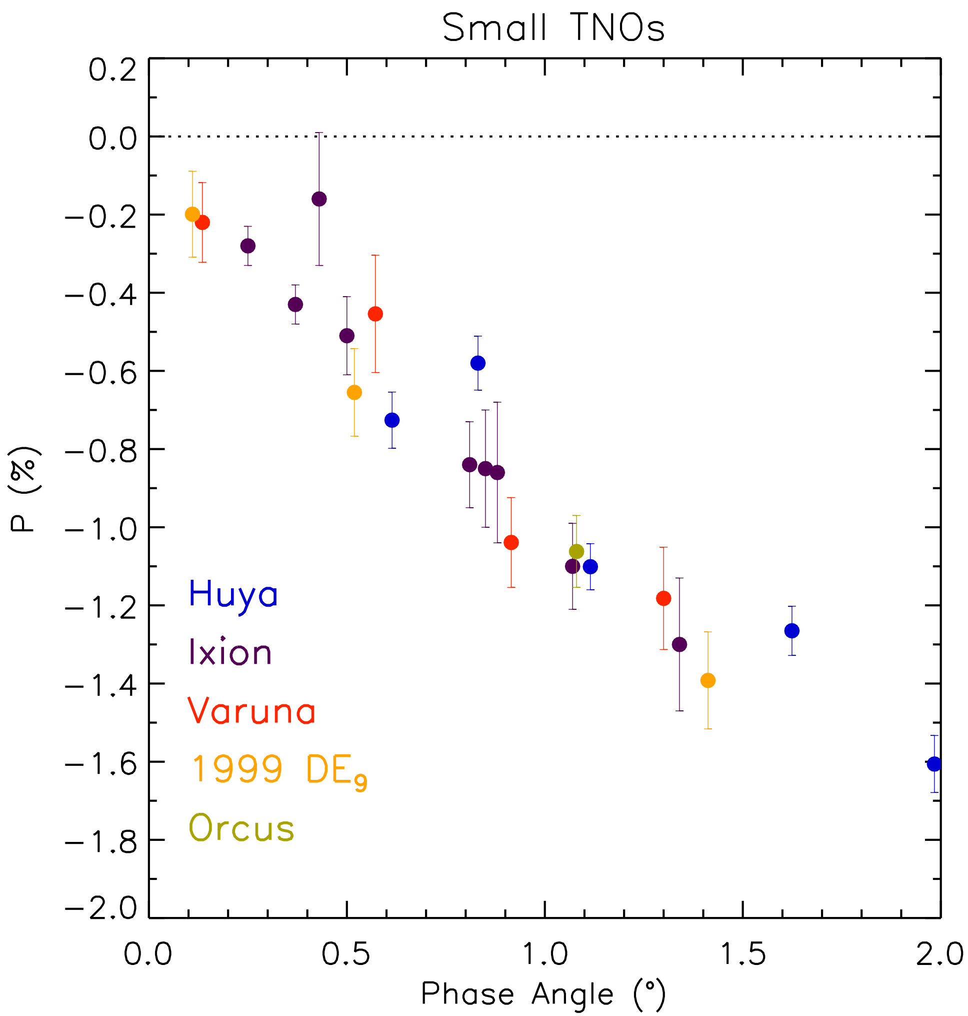

Bus-DeMeo Taxonomy Key

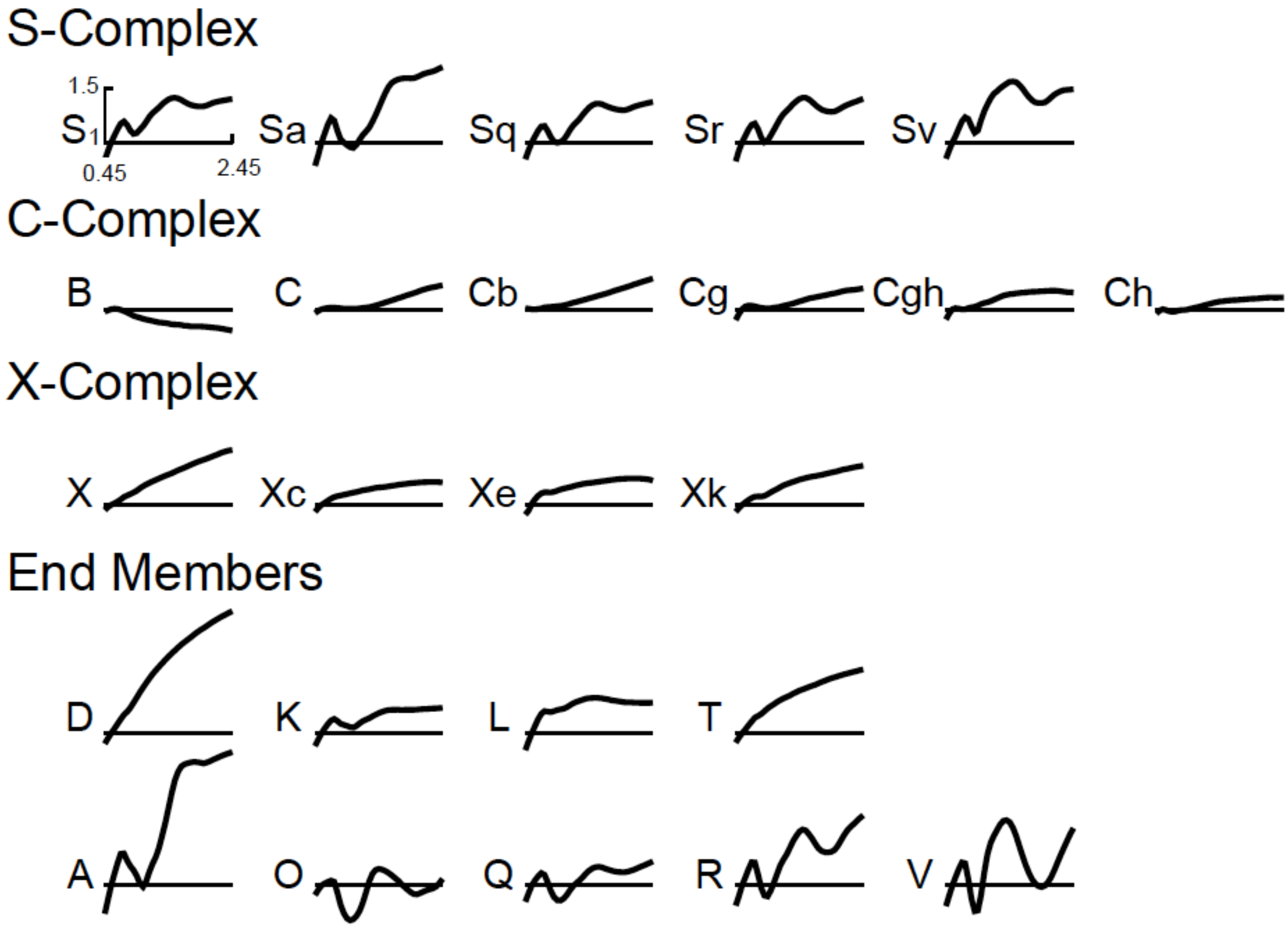

Bus-DeMeo spectral classification system

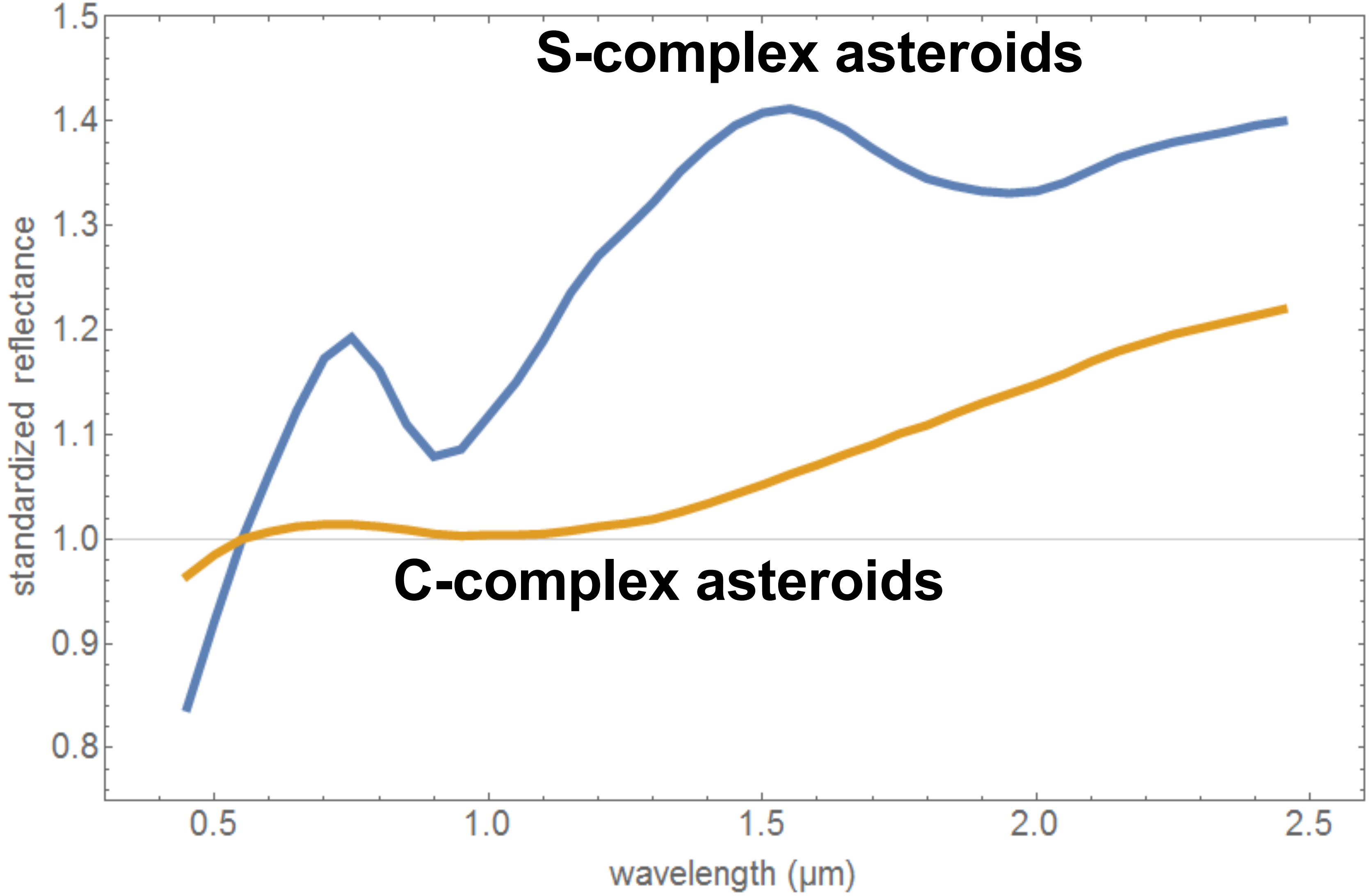

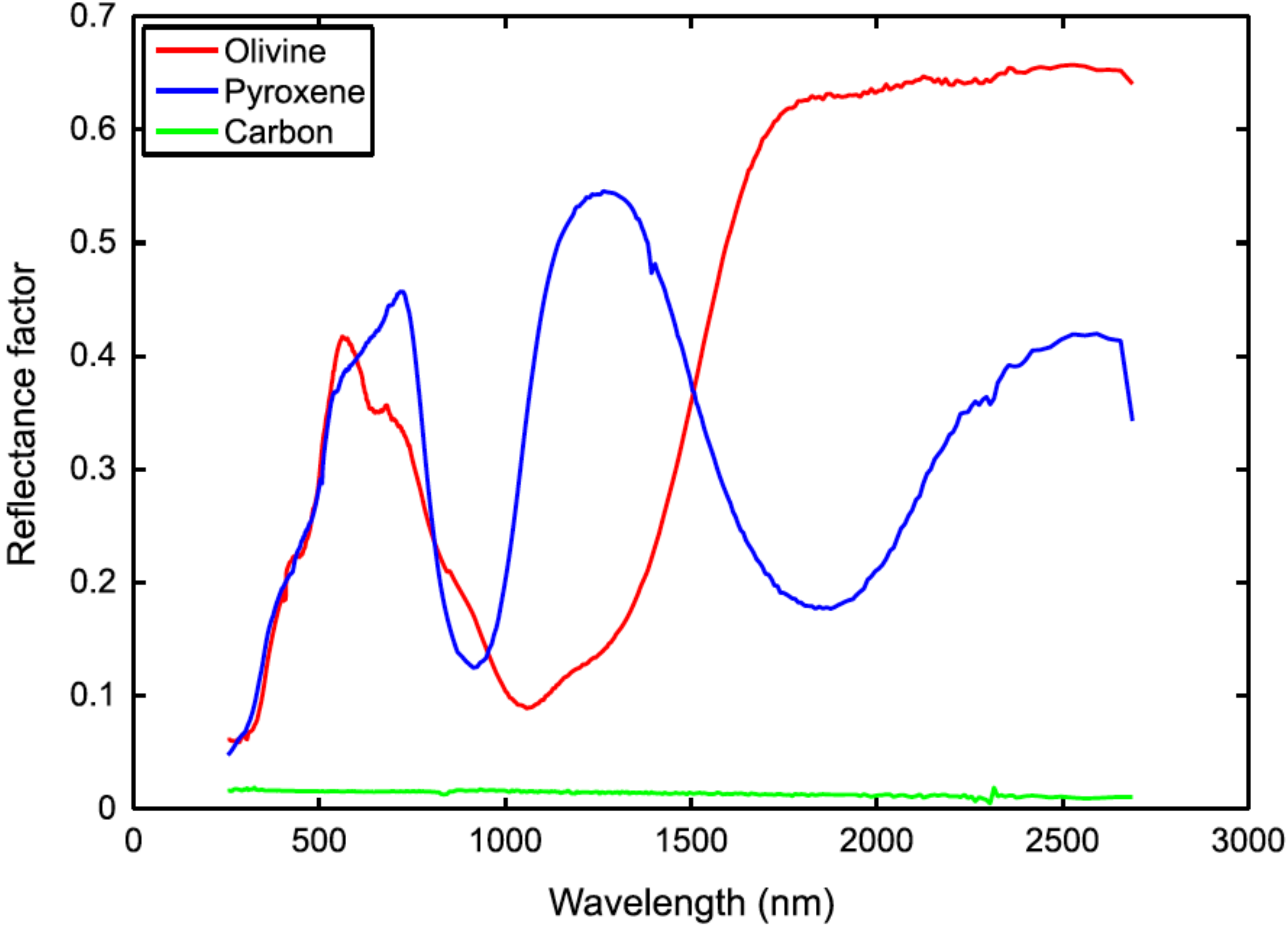

Olivine
Pyroxene
Carbon
Reflectance factor
Wavelength (nm)
0
0.1
0.2
0.3
0.4
0.5
0.6
0.7
0
500
1000
1500
2000
2500
3000

(4) Vesta Vis-NIR spectroscopy

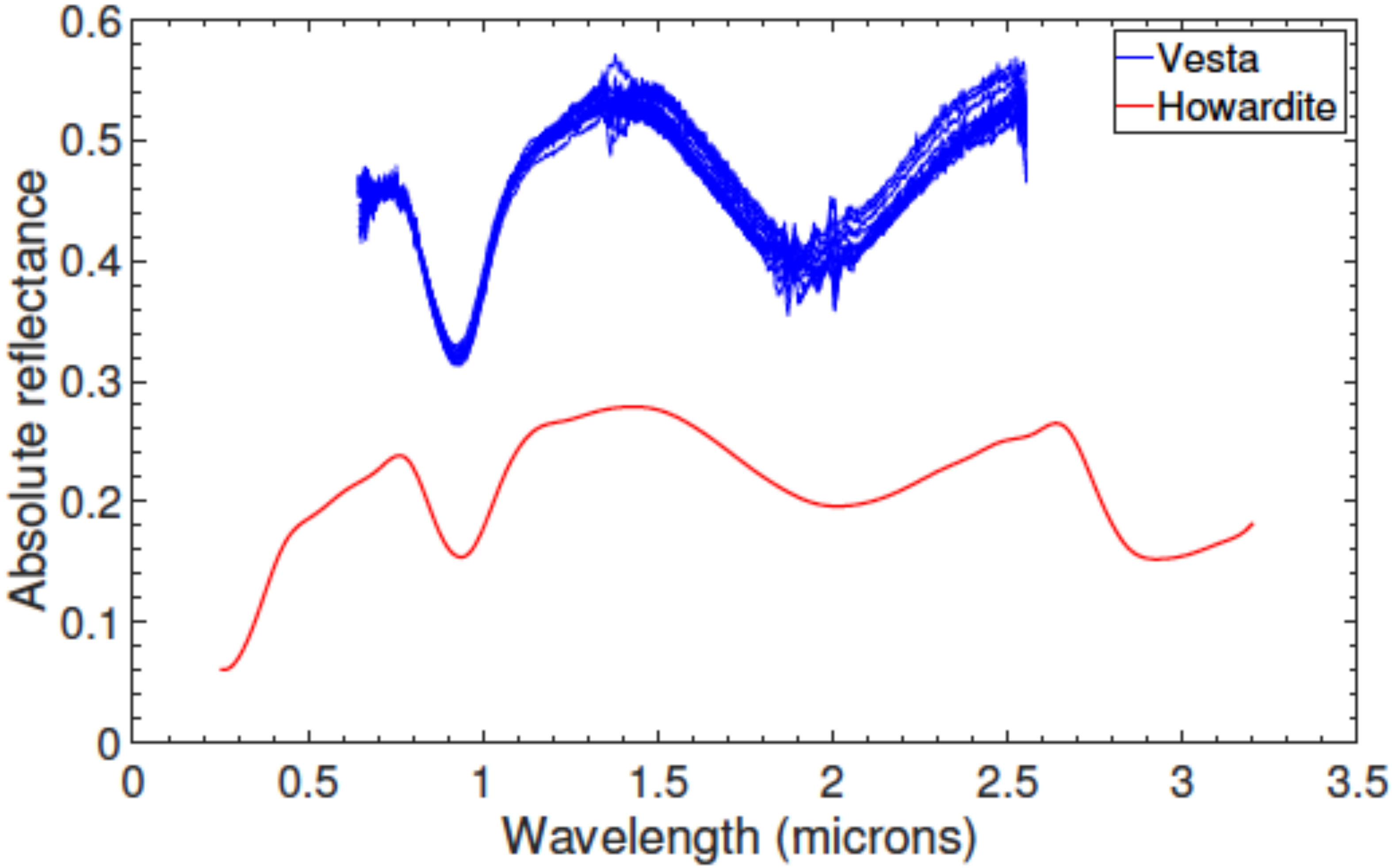

Martikainen et al. 2018, Reddy 2011

Multiple scattering

- Radiative transfer and coherent backscattering (RT-CB; Muinonen et al., ApJ 2012; Muinonen, WRM 2004 and URSI EMTS 1989)
- Superposition *T*-Matrix Method (STMM or MSTM; Mackowski & Mishchenko, JQSRT 2011; FaSTMM, Markkanen & Yuffa JQSRT 2017)
- Electric Current Volume Integral Equation Method (JVIE; Markkanen & Yuffa, JQSRT 2017, Markkanen et al., IEEE-TAP 2012)
- Radiative transfer with reciprocal transactions (R^2T^2; Muinonen et al., URSI EMTS 2016ab, RS 2017, OL 2018, JoVE 2019; Markkanen et al., OL 2018, ApJL 2018; Väisänen et al., PLoS ONE 2019)

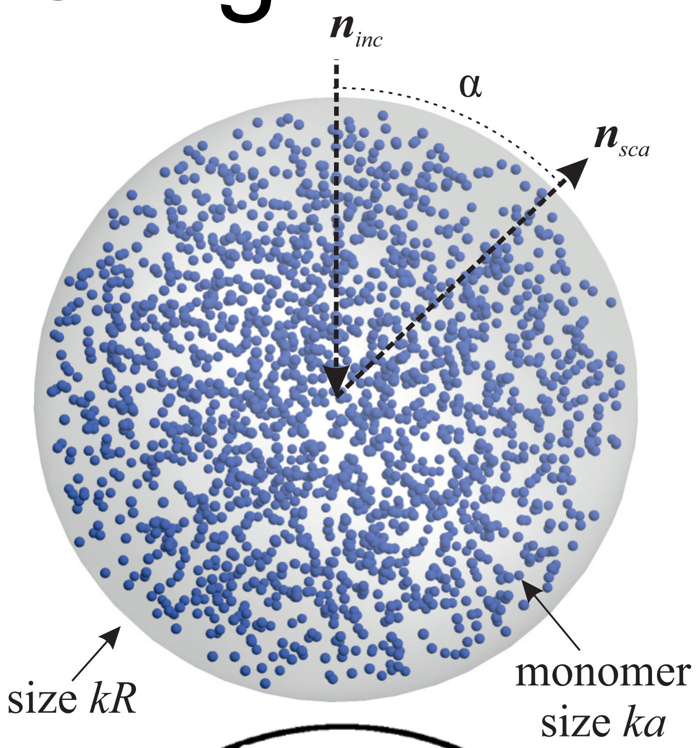

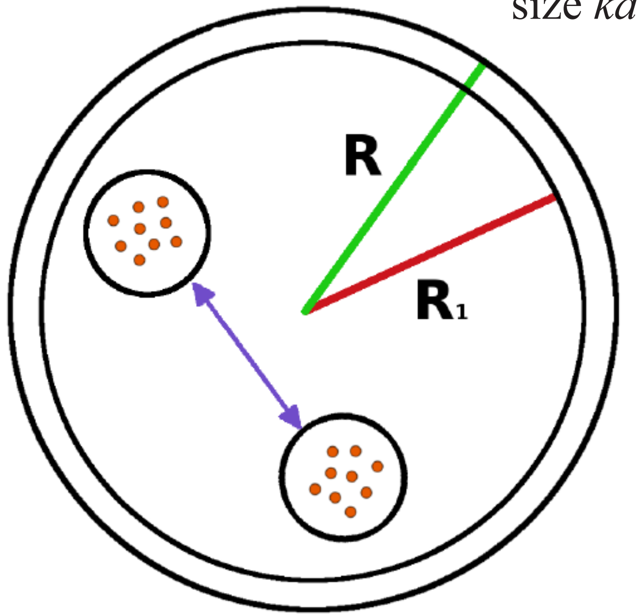

Different methods e.g., IEM, DEC, FEM, STMM, ...

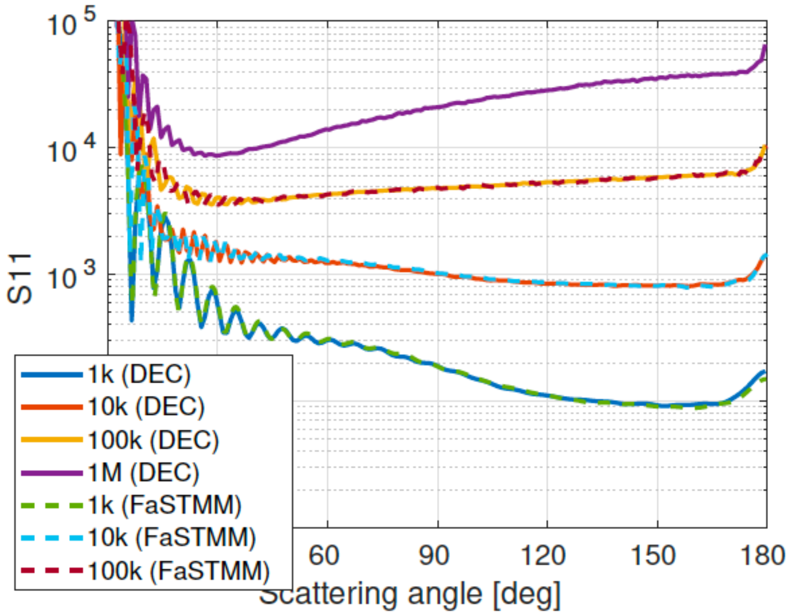

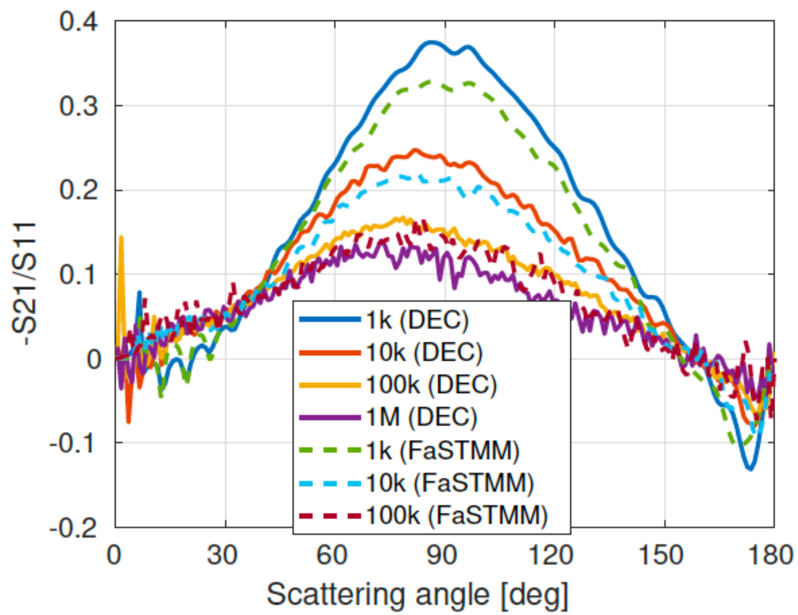

Spherical medium of randomly positioned spheres: $r = 0.18$ µm, $\epsilon_r = 2.25 + 0.0003i$, $\rho = 0.2$, $\lambda = 0.649$ µm

size	#particles	unknowns	cores	wall time	total cpu time
$R = 3.1$ µm	1k	9.6M	192	11 s	0.6 h
$R = 6.7$ µm	10k	66M	576	30 s	4.9 h
$R = 14.4$ µm	100k	550M	576	800 s	130 h
$R = 31.1$ µm	1000k	5000M	4096	2000 s	2400 h

CPU time $\sim R^4$

Order-of-scattering expansion

$$\mathbf{E}^{sca} = \sum_i \mathbf{G}\hat{\mathbf{T}}_i\mathbf{E}^{inc} + \sum_{i,j\neq i} \mathbf{G}\hat{\mathbf{T}}_i\mathbf{G}\hat{\mathbf{T}}_j\mathbf{E}^{inc} + \sum_{i,j\neq i,k\neq j} \mathbf{G}\hat{\mathbf{T}}_i\mathbf{G}\hat{\mathbf{T}}_j\mathbf{G}\hat{\mathbf{T}}_k\mathbf{E}^{inc} + .$$

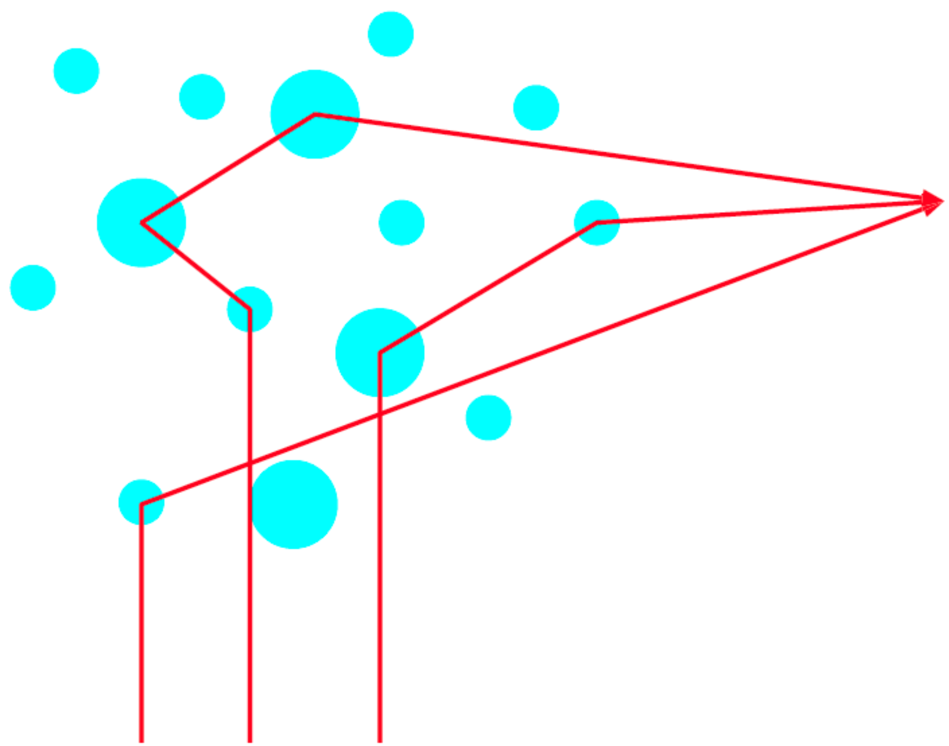

$\hat{\mathbf{T}}$ transition dyadic: $\mathbf{E}^{inc} \rightarrow \mathbf{J}$

$\mathbf{G}$ Green's dyadic operator: $\mathbf{J} \rightarrow \mathbf{E}^{sca}$

Discrete random media: Ensemple averaged coherency dyadic

$$< \mathbf{E}(\mathbf{r}) \otimes \mathbf{E}(\mathbf{r}) >=< \sum_i \mathbf{G}\hat{\mathbf{T}}_i \mathbf{E}^{inc}(\mathbf{r}') + \sum_{i,j\neq i} \mathbf{G}\hat{\mathbf{T}}_i \mathbf{G}\hat{\mathbf{T}}_j \mathbf{E}^{inc}(\mathbf{r}') + \ldots$$

$$\otimes \sum_k \mathbf{G}\hat{\mathbf{T}}_k \mathbf{E}^{inc}(\mathbf{r}'') + \sum_{k,l\neq k} \mathbf{G}\hat{\mathbf{T}}_k \mathbf{G}\hat{\mathbf{T}}_k \mathbf{E}^{inc}(\mathbf{r}'') + \ldots >$$

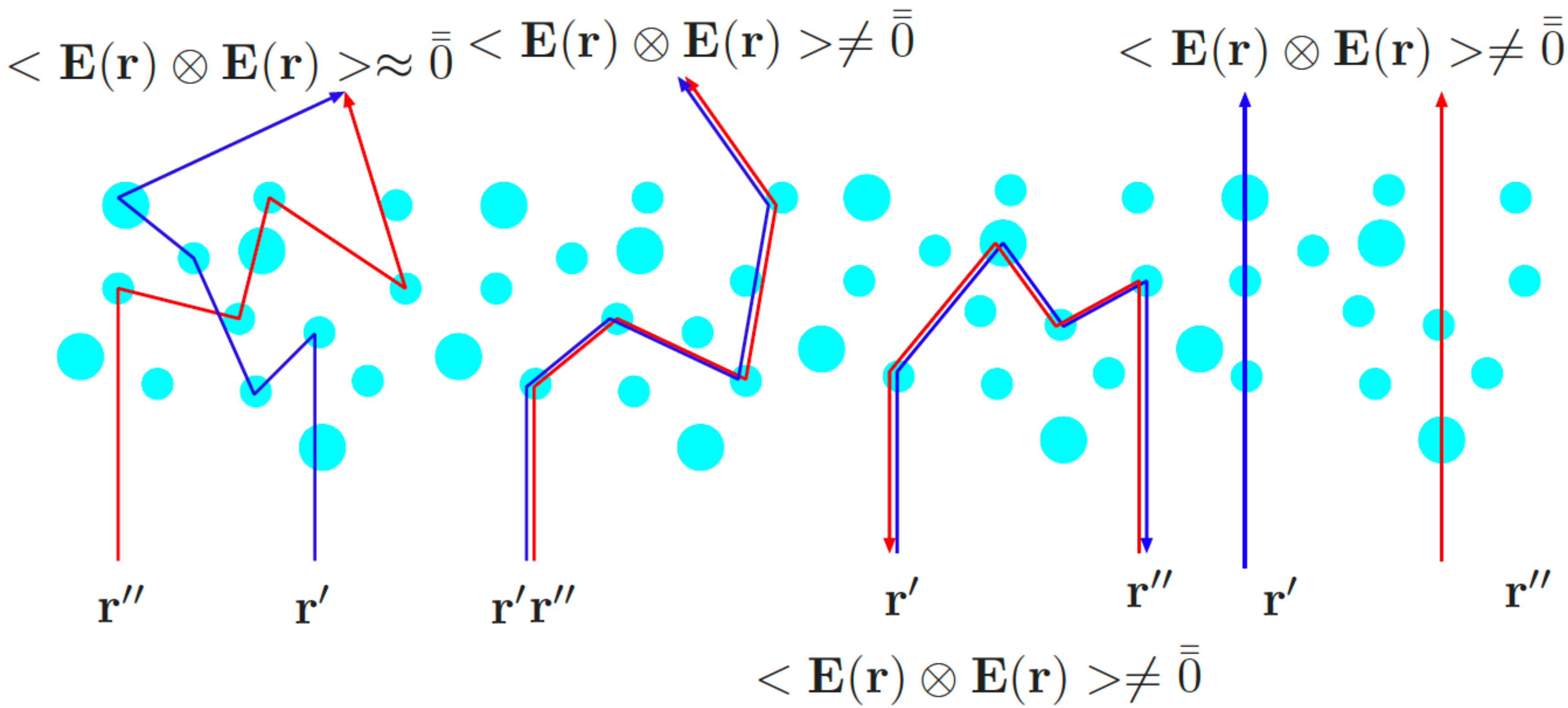

Coherent backscattering mechanism: intensity

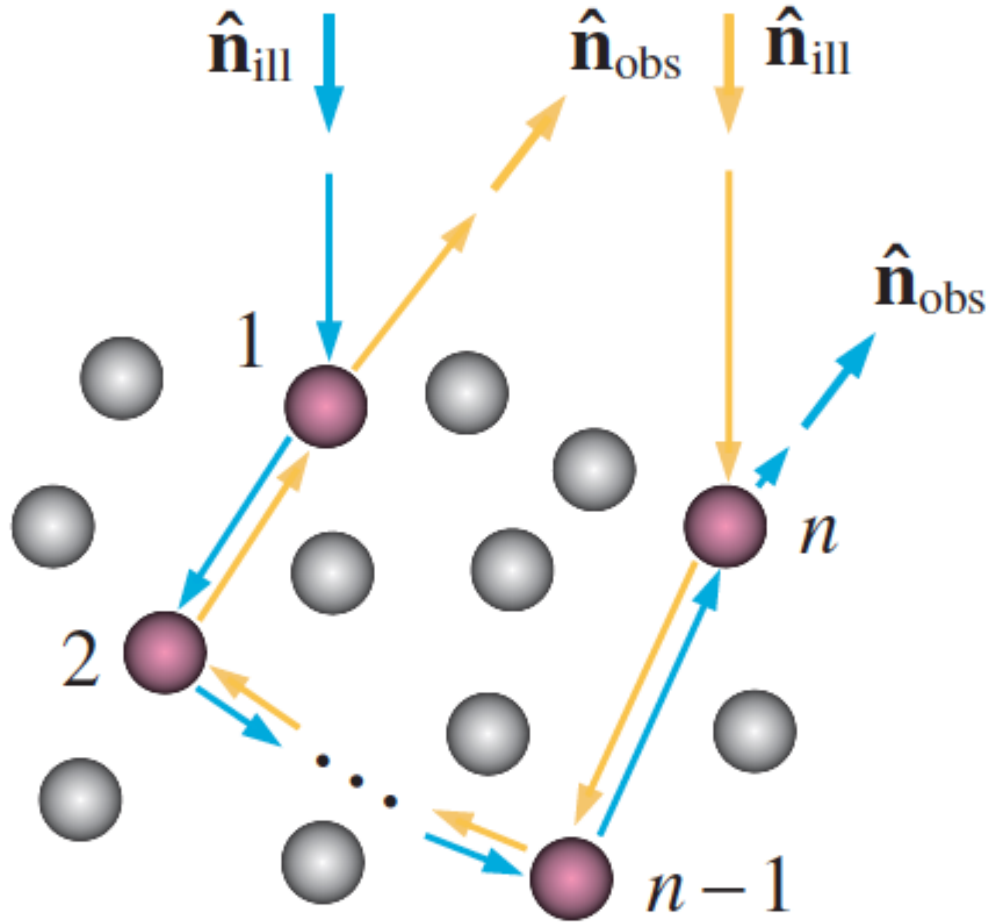

e.g., Muinonen 1989, 1990; Shkuratov 1985, 1988, 1989

Coherent backscattering mechanism: polarization

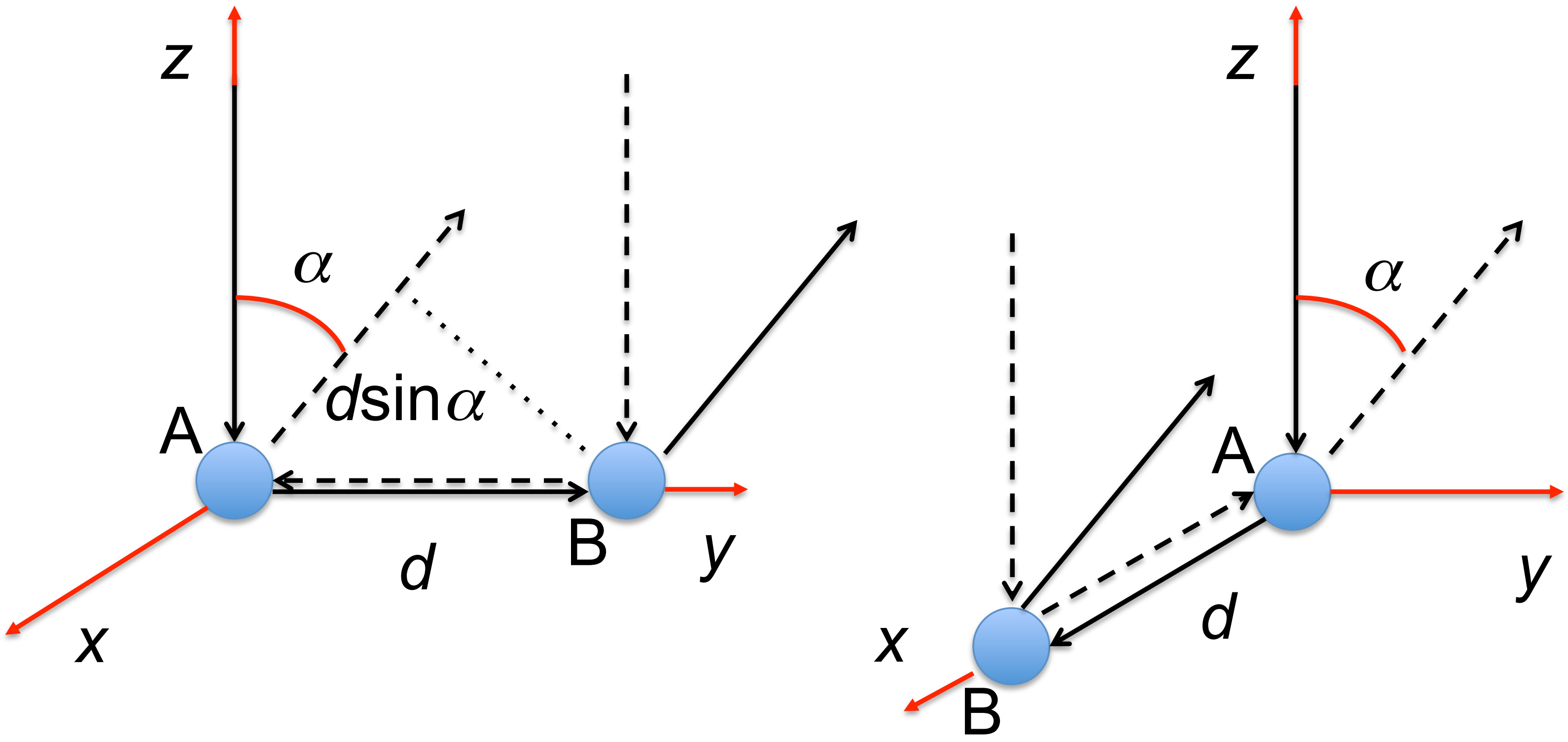

Muinonen 1989, 1990; Shkuratov 1985, 1988, 1989

Astrophysical Scattering Laboratory

- Novel scattering instrumentation

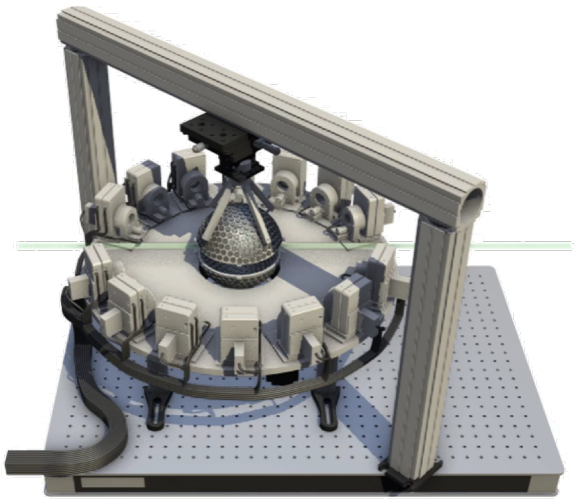

Scatterometer, visual wavelengths

Spectropolarimetric goniometer for surface BRDF, from 0.420 µm to 0.9 µm

Integrating-sphere reflectance (or transmittance) spectrometer, from 0.250 µm to 3.2 µm

Scatterometer

Measuring full angular Mueller matrix for scattering, at cm to sub-mm scales and multiple visual wavelengths. The sample is levitated and rotated with ultrasound, as well as 3D-modeled at the same time.

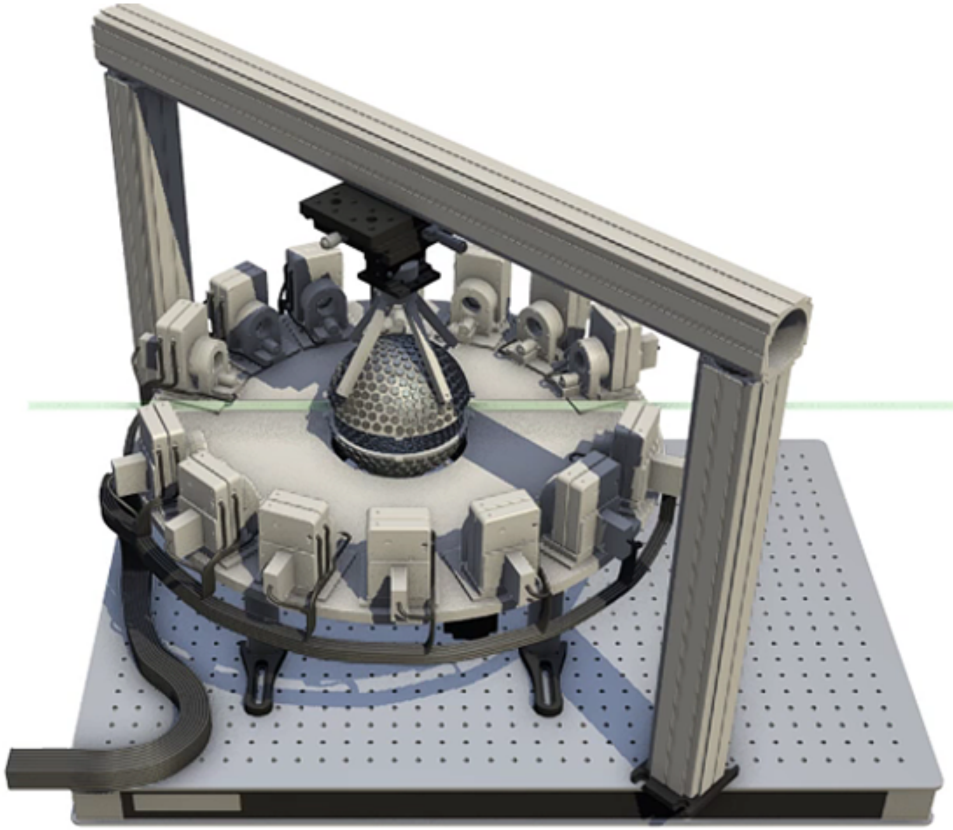

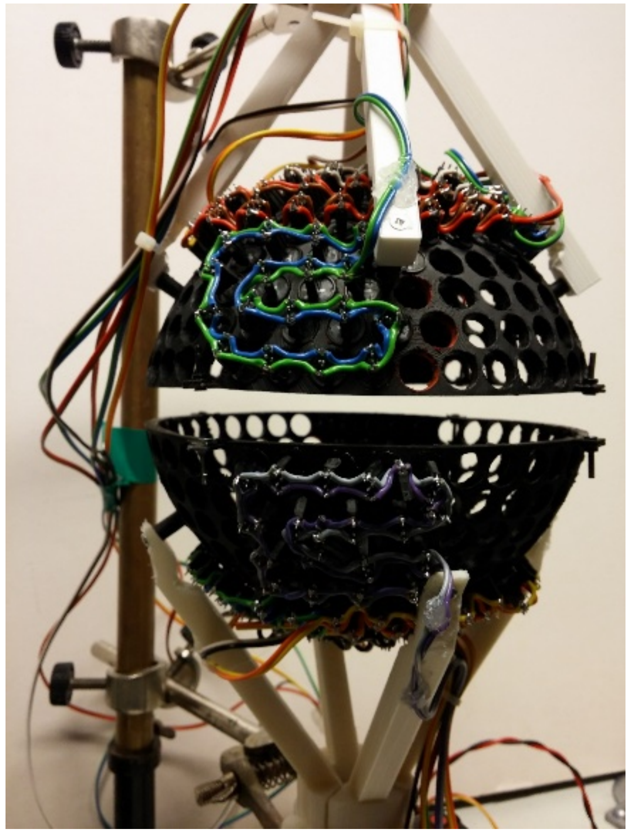

Maconi et al. JQSRT 2018

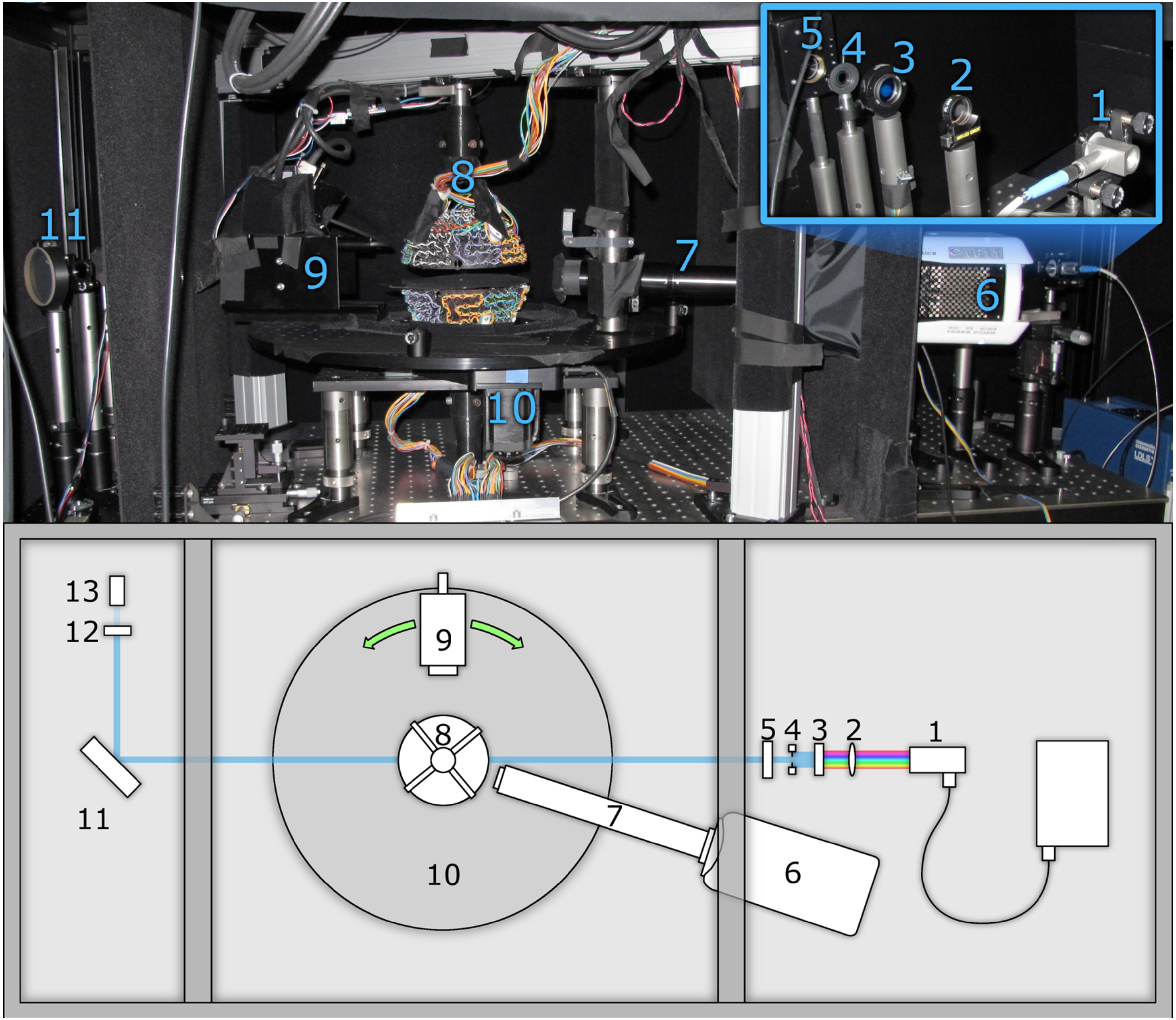

5
4
3
2
1
11
9
8
7
6
10
13
12
11
9
8
5 4 3 2 1
7
6
10


Orginal 100fps
3x speed
2mm

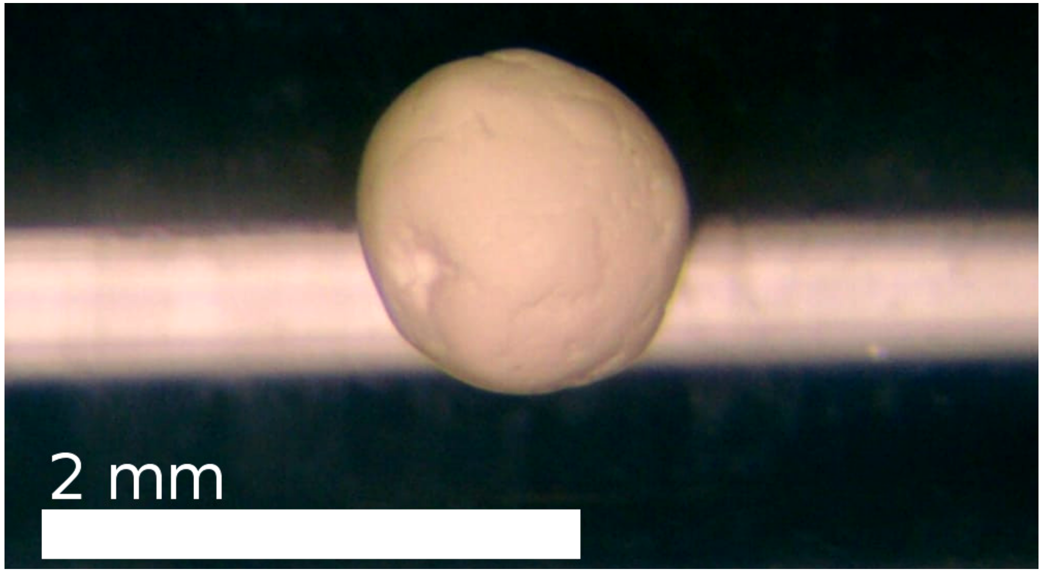

Muinonen et al.,
JoVE 2019

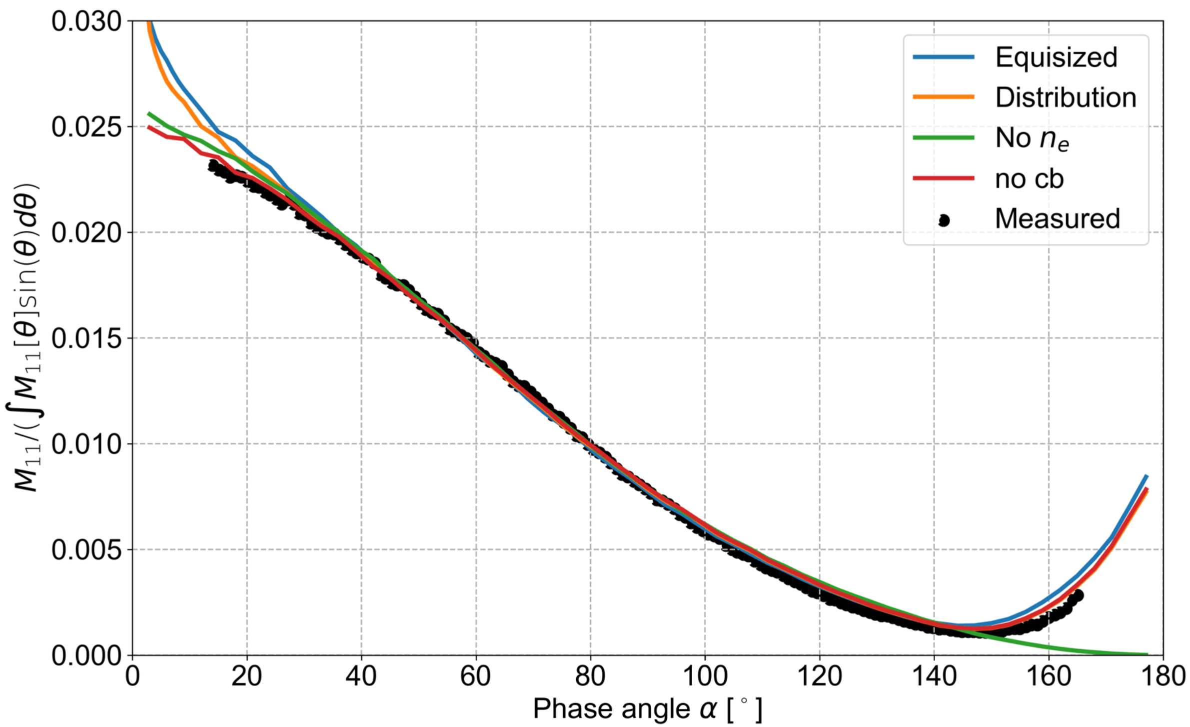

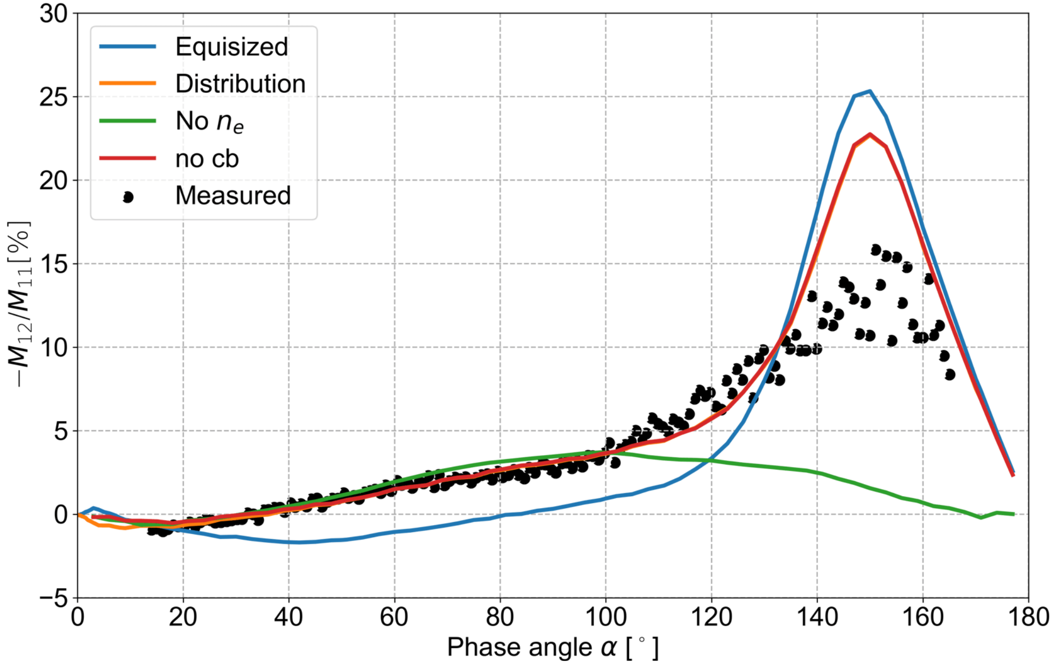
Equisized
Distribution
No n_e
no cb
Measured
$-M_{12}/M_{11}\,[\%]$
Phase angle α [$^\circ$]
30
25
20
15
10
5
0
−5
0
20
40
60
80
100
120
140
160
180

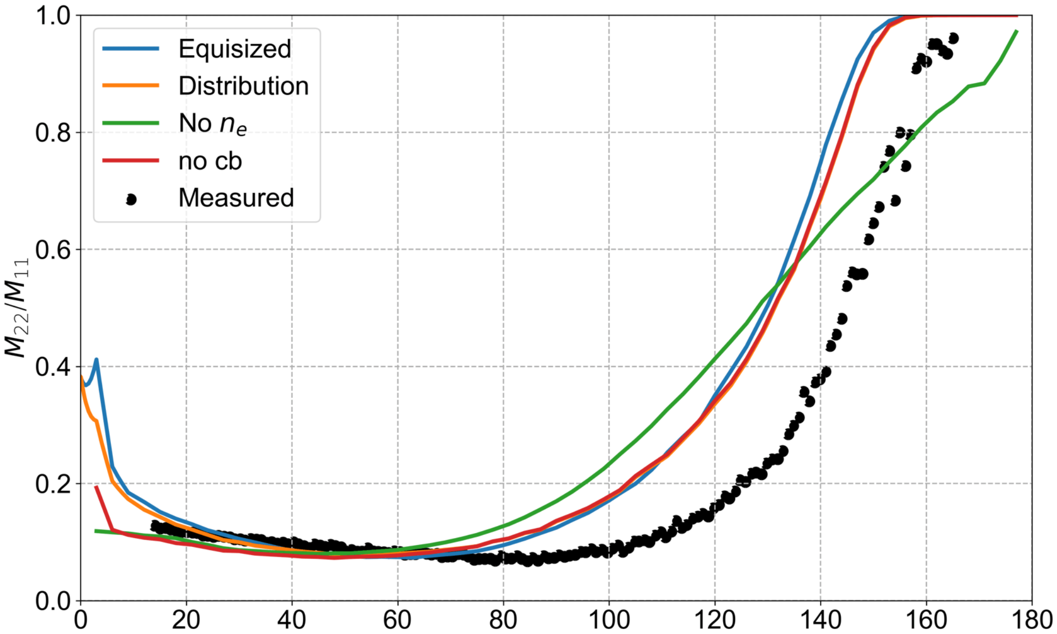
Equisized
Distribution
No n_e
no cb
Measured
M_{22}/M_{11}
1.0
0.8
0.6
0.4
0.2
0.0
0
20
40
60
80
100
120
140
160
180